

Auger coefficient of GaP(Zn, O). II. Evaluation from the temperature dependence of the luminescence efficiency

G. F. Neumark, D. J. DeBitetto, R. N. Bhargava, and P. M. Harnack

Philips Laboratories, Briarcliff Manor, New York 10510

(Received 26 July 1976)

Measurements have been made of the luminescence efficiency of several *p*-GaP(Zn, O) samples as a function of temperature. The relative variation of the efficiency is known to depend both on the Auger effect at the (Zn, O) center and on the fraction of excitation lost through alternate paths. Arguments are presented that the loss to alternate paths should be relatively independent of temperature. This is confirmed by comparison with data on the luminescent decay time. Consequently, we can obtain values of the Auger coefficient from the measurements. The exact value depends on the Hall factor and on the role of screening, but is within the range $(2-5) \times 10^{-11}$ cm³/sec.

I. INTRODUCTION

The efficiency of luminescent materials is of interest not only for practical applications, but also for an understanding of the microscopic recombination processes. We have studied the variation of the luminescence efficiency of the exciton emission of the Zn-O nearest-neighbor complex in GaP as a function of temperature from 77°K to room temperature. This was performed on several samples, with doping ranging from N_A of 0.5×10^{18} to 2×10^{18} cm⁻³. Measurements of the Hall effect and of the luminescent time decay of these same samples were also taken. This latter work has been reported earlier.¹ It was shown¹ that despite improved information on quantities required in the evaluation—such as the Hall coefficient and the hole activation energy—there is still some uncertainty in transition parameters because of inadequate knowledge of both the Hall factor and of screening effects.

A specific aim of the present analysis was an improved evaluation of the nonradiative Auger contribution. The earlier¹ work on time decay determined this contribution only to within an order of magnitude, primarily because of uncertainty surrounding screening effects. The uncertainty in the Auger effect has now been reduced to a factor of about 2. In addition, the results give further insight into factors determining the efficiency.

The data and previous¹ results relevant to the present work are presented in Sec. II, followed by an improved derivation of the luminescence efficiency in Sec. III. The results of Sec. III are applied to the data in Sec. IV, and the conclusions are discussed in Sec. V.

II. DATA AND REVIEW OF DECAY RESULTS

The relative luminescence efficiency of the *p*-GaP(Zn, O) epitaxial samples studied in Ref. 1,

namely, layers 120, 163, and 124, was measured as a function of temperature. The results are shown in Fig. 1, normalized to the same value at 77°K. The Zn doping of these layers varied from N_A of 0.5×10^{18} to 2×10^{18} cm⁻³. The specific concentrations, as obtained from the Hall data (Ref. 1), were $N_A = 0.5 \times 10^{18}$, 1.2×10^{18} , 2×10^{18} cm⁻³, and $N_D/N_A = 0.25$, 0.20, and 0.25 for layers 120, 163, and 124, respectively.

In the measurement of the efficiency, the input power was carefully monitored by use of a reference beam. The 5145-Å multimode beam from an argon laser was divided into two beams at a double prism. Both beams were alternately interrupted by a slowly rotating semicircular shutter. The first beam was spread in one direction by a cylindrical lens so that the entire area of the sample used in the Hall measurements was illuminated

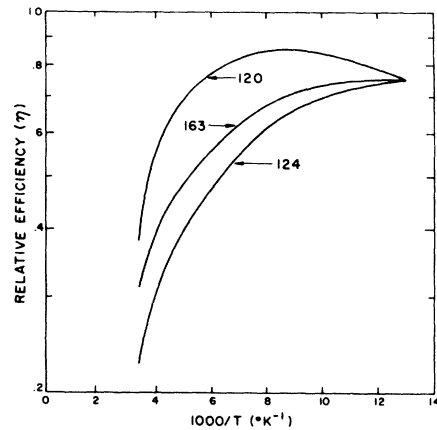


FIG. 1. Relative photoluminescent efficiency as a function of temperature. The curves for the different layers are normalized to the $T = 77$ °K value. The doping of the samples is $N_A = 0.5 \times 10^{18}$, 1.2×10^{18} and 2×10^{18} , $N_D/N_A = 0.25$, 0.20, and 0.25 for layers 120, 163, and 124, respectively.

(other parts of the sample were covered with absorbing paint). The emission from the sample passed through a double-prism beam splitter, a red hi-pass filter (Corning 2-64), and then onto an S-20 photomultiplier. The output from the photomultiplier was amplified and recorded on a strip chart ($x-t$) recorder. Linearity of the detection-recorder system was also verified. The second beam, the reference beam, was directed to strike a chip of GaP kept at room temperature. Radiation from the monitor chip was detected on alternate half cycles of the chopper, using the identical detection, amplification, and recording components as for the sample radiation. The strip record therefore presented a monitor of the sample input laser power and of the stability of the detection recording system, interlaced with the output signal throughout the temperature run. Corrections were made whenever the signal from the monitor sample changed. The monitor corrections required were always less than 10% of the signal.

The "test" sample was mounted on a copper block inside a glass Dewar, as described in Ref. 1. The temperature dependence of its luminescence was measured in the range of 77–300°K.

In addition to the measurement of the efficiency versus temperature for the red luminescence (described above), the spectral emission of layer 120 was measured at 77°K. It was found that the intensity of the green luminescence was $\approx 1\%$ that of the red.

Measurements of both the Hall effect and of the luminescent decay rate of these same layers (again as a function of temperature) were also taken, and have been reported previously.¹ It was pointed out in Ref. 1 that the interpretation of these measurements was complicated by two aspects: (i) uncertainty in the hole concentration (p) because of uncertainty in the Hall factor ($r \equiv \mu_H/\mu_D$), and (ii) uncertainty in the transition probabilities, since their dependence on screening has not been adequately determined. These uncertainties also apply to the analysis of the efficiency. Nevertheless, in the earlier¹ work it was shown that the uncertainty in p is less serious than that in the transition probabilities. For a reasonable range of the Hall factor, the resultant variation in the Auger coefficient (B) was only $\sim 70\%$, whereas for the transition probability problem, it was a factor of 3. In the analysis of the temperature dependence of the efficiency we shall, therefore, primarily use a Hall factor of unity. A brief discussion for other values of r is, however, given in Sec. IV B.

In a part of the present analysis we also require the occupancy factor of the exciton-hole level (f). This was calculated in the prior work¹; values for

the case of screening-independent transition probabilities are listed in Table I.

III. THEORY

A. Recombination equations

The transitions we are considering for the present analysis are shown in Fig. 2. They are slightly modified in one respect from those given earlier¹ for the analysis of the decay: a "shunt"²⁻⁴ path must be included. We define this shunt path to include all decay processes other than through the exciton center; namely, the customary²⁻⁴ unknown nonradiative recombination, the ir luminescence, the green luminescence, etc. However, we expect that in the present samples the dominant shunt process is the nonradiative path. As in Ref. 1, we restrict the analysis to $T \leq 250^\circ\text{K}$, so that electron thermalization can be neglected. Note that under this condition, the shunt path will not affect the decay from the exciton center—which is the reason for neglecting this path in Ref. 1.

The derivation of the kinetic and efficiency equations for systems such as that of Fig. 2 is well established by now²⁻⁴:

$$\frac{dn}{dt} = G - n(N_t - N_t^e)v\sigma_e - \frac{n}{\tau_s}, \quad (1)$$

$$\frac{dN_t^e}{dt} = n(N_t - N_t^e)v\sigma_e - N_t^e \left[f \left(\frac{1}{\tau_{xr}} + Bp \right) \right], \quad (2)$$

$$\eta = fN_t^e/G\tau_{xr}. \quad (3)$$

Here η is the efficiency; G is the excitation intensity; n and p are the electron and hole concentrations, respectively; N_t and N_t^e are the concentrations of exciton centers and of such centers filled with electrons, respectively; v is the thermal velocity; σ_e is the capture cross section of an electron into the exciton center; τ_s is the decay constant of the shunt path; and f , τ_{xr} , and B are as defined in Ref. 1.

Since we are interested in the efficiency, a steady-state quantity, the time derivatives vanish. With the defining equations

$$\tau_{nt} = (N_t v \sigma_e)^{-1}, \quad (4)$$

$$1/\tau_\alpha = f(1/\tau_{xr} + Bp), \quad (5)$$

solution of Eqs. (1)–(3) for $dn/dt = dN_t/dt = 0$ gives

$$2\eta = \frac{1}{1 + Bp\tau_{xr}} + \frac{fN_t}{G\tau_{xr}} \left(1 + \frac{\tau_{nt}}{\tau_s} \right) - \left\{ \left[\frac{1}{1 + Bp\tau_{xr}} + \frac{fN_t}{G\tau_{xr}} \left(1 + \frac{\tau_{nt}}{\tau_s} \right) \right]^2 - \frac{4fN_t}{G\tau_{xr}} \left(\frac{1}{1 + Bp\tau_{xr}} \right) \right\}^{1/2}. \quad (6)$$

TABLE I. Exciton occupancy factor.

Temperature (°K)	f		
	Layer 120	Layer 163	Layer 124
77	0.02 ₅	0.06	0.08
100	0.05 ₅	0.11	0.15
125	0.09	0.15	0.19
150	0.11	0.20	0.21
175	0.12	0.20	0.24
200	0.12 ₅	0.21	0.25
225	0.13	0.22	0.27
250	0.13	0.22	0.27
275	0.12	0.21	0.26
300	0.11	0.20	0.25

Over most of the range of the present measurements, the excitation intensity (G) is low enough so that

$$N_t^e/N_t \ll 1, \quad (7)$$

where it is easy to show that condition (7) follows, provided

$$G\tau_\alpha/N_t \ll 1 + \tau_{nt}/\tau_s. \quad (8)$$

The corresponding solution for this case is

$$\eta = [(1 + \tau_{nt}/\tau_s)(1 + Bp\tau_{xr})]^{-1}. \quad (9)$$

Let us now consider the physics of the efficiency degradation as given in Eqs. (6) and (9), to clarify the subsequent treatment. First, the origin of the degradation for the low intensity case, Eq. (9), is easily understood²⁻⁴ as a consequence of two effects: (i) the Auger nonradiative contribution (Bp); here, as the hole concentration increases with temperature, the efficiency degrades; and (ii) the

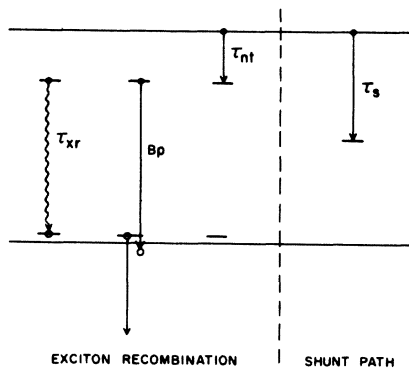


FIG. 2. Schematic of the transitions used in the present analysis. The radiative transition at the (Zn,O) center has a rate $1/\tau_{xr}$, the Auger recombination is proportional to the Auger coefficient (B) times the hole concentration (p), and the rate of the shunt path is given by $1/\tau_s$. The rate of capture into the exciton center is $1/\tau_{nt}$.

recombination via the shunt path; this depends on the ratio of the capture time into the exciton center (τ_{nt}) to the decay constant of the shunt path (τ_s), or specifically, on $(1 + \tau_{nt}/\tau_s)^{-1}$, the "branching ratio." Second, note that since Eq. (9) corresponds to the low-intensity case, differences between Eqs. (6) and (9) will occur for high-excitation intensities. In this range, one obtains "saturation" of the (Zn,O) centers, i.e., the number of filled exciton centers becomes comparable to the number of total exciton centers ($N_t^e/N_t \sim 1$). Since filled centers cannot capture conduction electrons, the exciton path gets "blocked." Moreover, on the model of Eq. (1), the shunt path does not saturate (it is assumed to maintain a constant decay time τ_s); consequently, more electrons now flow through this path, degrading the efficiency. Of relevance to our analysis (Sec. IV C) is the fact that since lower occupancy factors lead to slower exciton decay, the saturation at a given excitation level increases with decreasing f [Eq. (6) is expressed in terms of f/G]. Consequently, in this regime lower occupancy factors lead to lower efficiencies.

B. Temperature dependence of η

In analyzing the temperature dependence of the efficiency via Eqs. (6) or (9), knowledge of the temperature variation of the various parameters is required. The hole concentration (p) has been measured, and the occupancy factor (f) has been evaluated previously¹ (Table I). Of the remaining parameters, τ_{nt} and τ_s occur only in the combination $(1 + \tau_{nt}/\tau_s)$. Moreover, the relative efficiencies as a function of T are approximately independent of $(1 + \tau_{nt}/\tau_s)$ if either (i) $\tau_{nt}/\tau_s \ll 1$, or (ii) τ_{nt}/τ_s is approximately independent of temperature. We have not been able to obtain much information on the second of these conditions, but the first one appears to hold. This is indicated for example by results of Henry *et al.*⁵ who find that for annealed samples at room temperature $\tau_{nt}/\tau_s \approx 0.3$. Similar conclusions about the dominance of the exciton path have been reached by Van der Does de Bye *et al.*^{6,7} from minority-carrier lifetime studies. Since our samples are expected to correspond approximately to annealed samples, it seems reasonable to assume that the relation $\tau_{nt}/\tau_s \ll 1$ applies, at least at room temperature. If this relation then persists also to lower temperature, it follows that $1 + \tau_{nt}/\tau_s \approx 1$ and this term will then be approximately independent of temperature. Information on this aspect can be obtained by simultaneous analysis of efficiency and of time decay data⁷ in the nonsaturated case [Eq. (9)].

Comparison of the decay equation [Eq. (1) of Ref. 1] with Eq. (9) gives

$$1 + \tau_{nt}/\tau_s = f\tau/\eta\tau_{xr} \quad (10)$$

We estimate (Sec. IV D) that, for our layers, $(1 + \tau_{nt}/\tau_s)$ remains constant to about 20% in the temperature range of the analysis.

As for the temperature dependence of the remaining parameters in Eqs. (6) and (9), namely, τ_{xr} and B , if these do not depend on screening, they are expected to be almost temperature independent (Refs. 8 and 9). If they do depend on screening, one again (Ref. 1) has to consider the temperature variation of the Bohr radius. We now treat only the nonsaturated case [Eq. (9)] quantitatively, so that only the product $B\tau_{xr}$ is required

$$B\tau_{xr}/B_0\tau_{xr}^0 = (\beta/\beta_0)^2, \quad (11)$$

where β , β_0 , B_0 , and τ_{xr}^0 are defined in Ref. 1, and β/β_0 is again obtained from the results of Lam and Varshni.¹⁰

IV. ANALYSIS OF DATA

A. Further consideration of efficiency equations

It may at first appear difficult to evaluate the Auger coefficient from Eqs. (6) and (9) since a fair number of parameters are involved, many of them poorly known. Nevertheless, a meaningful analysis is obtained if the main effects are analyzed first, and corrections are made subsequently for second-order variations.

As a first step in emphasizing the main effects, one can use excitation intensities such that saturation effects are negligible over most of the range. The analysis can then be carried out with the simpler equation (9) rather than the full equation (6). To check on this simplification, we evaluate inequality (8): We estimate $G \approx 5 \times 10^{20}$ photons/cm³, $N_t \approx 2 \times 10^{15}$ cm⁻³ (Ref. 11); then, with $\tau_{xr} \approx 10^{-7}$ sec (Ref. 8), giving $G\tau_{xr}/N_t \approx 0.025$, with $f \approx 0.1$ (Table I), and neglecting $B\rho$, one obtains $G\tau_{xr}/N_t \approx G\tau_{xr}/fN_t \approx \frac{1}{4}$. Since f values for our layers are ≈ 0.1 over most of the range (Table I), Eq. (9) will mostly suffice. As a second step, we assume $(1 + \tau_{nt}/\tau_s)$ independent of temperature. Justification for this has been given in Sec. III. We present the results using both simplifications in Sec. IV B. The correction for saturation is then given in Sec. IV C, and the temperature dependence of $(1 + \tau_{nt}/\tau_s)$ is considered in Sec. IV D.

B. Analysis without saturation; $(1 + \tau_{nt}/\tau_s)$ independent of temperature

This case gives $\eta \sim (1 + B\rho\tau_{xr})^{-1}$; with ρ known, it is now simple, for given τ_{xr} , to fit to $\eta_{e,1}$ with

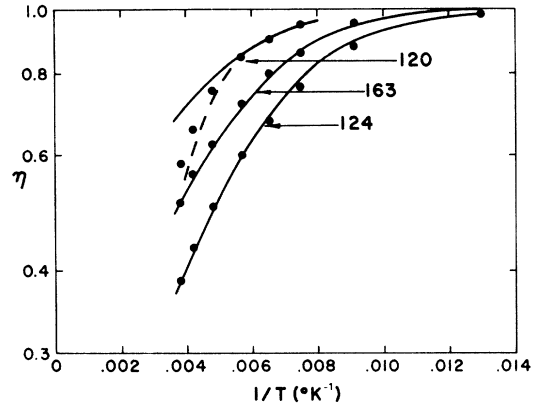


FIG. 3. Photoluminescent efficiency as a function of temperature. The circles are the experimental values. The lines are the fit with use of Eq. (9), $B = 2.3 \times 10^{-11}$ cm³/sec, and with transition probabilities independent of screening; the solid lines are for $(1 + \tau_{nt}/\tau_s)$ independent of temperature; the dashed line is for $(1 + \tau_{nt}/\tau_s)$ as given by Table II.

various values of B . Note, however, that τ_{xr} and B depend on the influence of screening (see Sec. III B).

The fit to the efficiency data, for the transition probabilities independent of screening, is shown in Fig. 3 (solid lines) with a value of $B = 2.3 \times 10^{-11}$ cm³/sec. The maximum observed efficiency has been fitted to the theoretical value, and the remaining data normalized. We estimate, from the fit at other values of B , that B is determined to within about 15%. The low-temperature data for layer 120 in the range where the efficiency decreases with decreasing temperature has been purposely omitted; this data is fitted in Sec. IV C, by including saturation effects. The fit for layers 163 and 124 is very good, and that for layer 120 reasonably good.

In connection with these results, a brief comment on the Hall-factor problem is in order (this aspect is otherwise neglected in the present paper). Within the approximations of this section, the efficiency is purely a function of the product $B\rho$. Consequently, the calculated value of B will be inversely proportional to the Hall factor. For example, the same fit can be obtained for Fig. 3 with $r = 0.7$, and $B = 3.3 \times 10^{-11}$ cm³/sec. (The analysis of Ref. 1 involves the value of f as well as the product $B\rho$, but a very comparable value, namely, $B = 3.5 \times 10^{-11}$ cm³/sec was obtained for this case.)

The results for the transition probabilities dependent on screening via Eq. (11) are given in Fig. 4 (solid lines) for $B = 3 \times 10^{-11}$ cm³/sec and in Fig. 5 for $B = 6 \times 10^{-11}$ cm³/sec. (Figures 4 and 5 show layers 120 and 124 only—as shown in Fig.

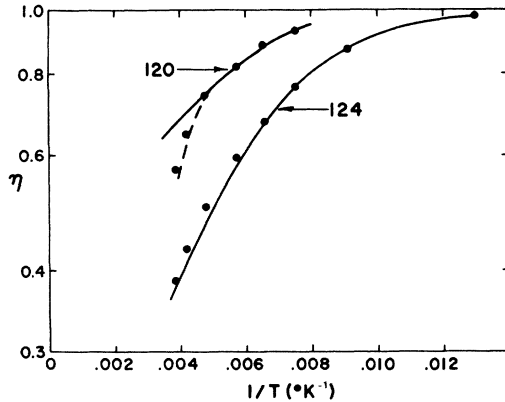


FIG. 4. Same as Fig. 3, but with the transition probabilities dependent on screening via Eq. (11), and $B = 3 \times 10^{-11}$ cm³/sec.

3, layer 163 behaves similarly to layer 124.) The fit in Fig. 4 is good (similar to that of Fig. 3), whereas that in Fig. 5 is poor. That latter value, $B = 6 \times 10^{-11}$ cm³/sec, interestingly, gave the best fit to the data in our analysis of the luminescence decay (Ref. 1). (This aspect is discussed further in Sec. V.)

C. Inclusion of saturation; $(1 + \tau_{nt}/\tau_s)$ independent of temperature

It can be seen from the data (Fig. 1) that at low temperatures ($\approx 110^\circ\text{K}$ down) the efficiency of layer 120 decreases with decreasing temperature. Assuming saturation, this can be explained by a decrease in the occupancy factor f with decreasing

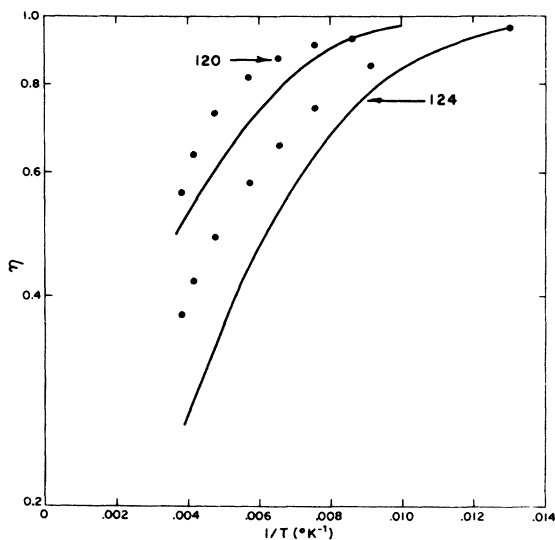


FIG. 5. Same as Fig. 4, but for $B = 6 \times 10^{-11}$ cm³/sec, and the fit with use of Table II (dashed line) omitted.

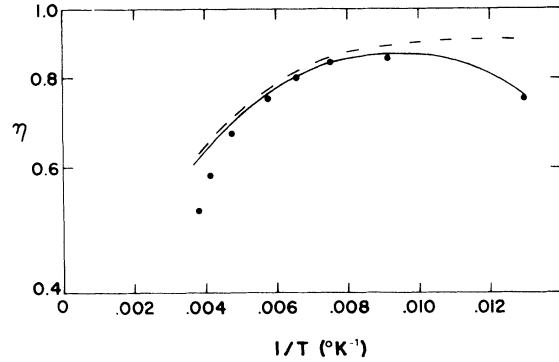


FIG. 6. Photoluminescent efficiency of layer 120 vs temperature. The circles are the experimental values. The solid line is the fit with use of Eq. (6), i.e., with inclusion of saturation of the (Zn,O) centers. Parameter values are $B = 2.3 \times 10^{-11}$ cm³/sec, $1 + \tau_{nt}/\tau_s = 1.1$, $G\tau_{xr}N_t = 2 \times 10^{-2}$, and f values as given in Table I. The dashed line gives the results obtained by use of Eq. (9).

temperature [see Eq. (6) and related discussion]. Such saturation effects *are* expected for this layer in the low-temperature range: with $G\tau_{xr}/N_t \approx 0.02$ (Sec. IV A), the 77°K value of $f = 0.025$ (Table I) leads to $G\tau_{\alpha}/N_t \approx 1$, and inequality (8) is thus not satisfied.

The results of an analysis based on Eq. (6), with the f values as given in Table I and for $G\tau_{xr}/N_t \approx 0.02$, $1 + \tau_{nt}/\tau_s = 1.1$ is shown in Fig. 6 as the solid line. The low-temperature fit can be seen to be good.

D. Role of τ_{nt}/τ_s

In the absence of saturation, the temperature dependence of $(1 + \tau_{nt}/\tau_s)$ is given by Eq. (10). For $T > 175^\circ$, saturation effects are negligible even for layer 120; in this range, the calculations for this layer with and without saturation (solid and dashed lines of Fig. 6) agree to 1% or better. Thus, for $T > 175^\circ$, one expects Eq. (10) to be valid. The resultant values of $(1 + \tau_{nt}/\tau_s)^{-1}$ are given in Table II, and it can be seen that this quantity remains essentially constant for layers 124 and 163. For layer 120 there is approximately

TABLE II. Temperature variation of branching ratio.

T (°K)	Normalized $(1 + \tau_{nt}/\tau_s)^{-1}$		
	Layer 120	Layer 163	Layer 124
175	1.00	1.00	1.00
200	0.94	1.01	1.00
225	0.84	0.96	0.97
250	0.79	0.95	0.97

a 20% decrease as the temperature increases. Moreover, the greater variation for layer 120 is to be expected, since this layer is likely to have a larger value to τ_{nt}/τ_s than the other layers: τ_{nt} decreases with increasing concentration of exciton centers N_i [Eq. (4)], and such centers would be expected to be more numerous in the more highly doped layers (163 and 124).

The consequence of the variation of $(1 + \tau_{nt}/\tau_s)$ for layer 120 is shown as the dashed line in Fig. 3, and now this layer also shows very good agreement with the observed values. Thus, the slight variation in $(1 + \tau_{nt}/\tau_s)$ explains why the fit for layer 120, considering only the Auger effect (Sec. IV B), was not as good as for layers 163 and 124. It should still be noted that similar corrections apply as well for screening-dependent transition probabilities, so that the fit for layer 120 in Fig. 4 can also be appropriately improved.

V. DISCUSSION AND CONCLUSION

A summary of the Auger coefficients obtained from the present work, as well as a comparison with those from the analysis of the decay (Ref. 1), is given in Table III (all values are for a Hall factor of unity).

The match to the data (Figs. 3, 4, and 6) with the Auger values as given in Table III is very good for layers 163 and 124 based on the simplest model, that of Sec. IV B (see Figs. 3 and 4), and is equally good for layer 120 provided one includes two reasonable corrections. These are the inclusions of saturation effects at low temperatures (Sec. IV C and Fig. 6) and a slight temperature variation of $(1 + \tau_{nt}/\tau_s)$ at the higher temperatures (Sec. IV D and dashed line in Figs. 3 and 4).

The remaining question is whether, given a particular case (e.g., that of unity Hall factor and screening-independent transition probabilities—Figs. 3 and 6), the fit is unique. In other words, can one obtain an equivalent fit by assuming a different saturation behavior, or a different temperature variation of $(1 + \tau_{nt}/\tau_s)$, and correspondingly

a different value of B ? If the saturation behavior of the layers is as postulated in Sec. IV C, i.e., saturation affects only layer 120 at low temperatures, we do expect that the fit is unique: it is obtained with values of $(1 + \tau_{nt}/\tau_s)$ which are *derived from independent (decay) data*—see Eq. (10) and Sec. IV D. Moreover, it is worth noting that a good fit is obtained with *three* different layers. Statements regarding the validity of the postulated saturation behavior have to be somewhat less categorical. Nevertheless, we feel plausibility arguments in favor are strong: the values used for quantitative estimates in Sec. IV C are very reasonable, and the overall approach is fully self-consistent. In addition, the good agreement of Table III (extremely good for screening-independent transition probabilities, acceptable for the screening-dependent case) in values of Auger coefficient as obtained via the present analysis of the efficiency and the earlier¹ analysis of the decay can hardly be regarded as a coincidence; this thus strongly confirms the present approach.

As we have just mentioned, the agreement in Auger coefficients (Table III) is better for screening-independent transition probabilities. This indicates that the transition probabilities in the present doping range may be independent of screening—or, more likely, vary less strongly than predicted from Eq. (11) and the results of Lam and Varshni.¹⁰ However, since the disagreement for this latter approach is not far out of line (3 ± 0.5 vs 6 ± 2), this conclusion is tentative.¹²

Regarding comparison of the present results with other values in the literature, it was only the present detailed results—with decay, relative efficiency, and hole concentration known at low temperatures where thermalization is negligible—which made an investigation of screening effects meaningful. The effect of screening on the energy levels is now well confirmed (see especially Sec. V of Ref. 1), although that on the transition probabilities is still in doubt. In some of the earlier work^{3,4} screening was considered empirically, but with an analysis which does not agree well with the present results on energy levels and transition probabilities (see especially Sec. II C of Ref. 1). The more recent work of Van der Does de Bye⁷ used the product $B\tau_{tr}$ in the analysis, and effectively assumed this independent of screening. In view of these differences, agreement between the present range, for unity Hall factor, of $B = (2-3.5) \times 10^{-11}$ cm³/sec (Table III), with the earlier values (also for unity Hall factor) of $B \approx 3 \times 10^{-11}$ cm³/sec (Refs. 3 and 7) and $B \approx 5 \times 10^{-11}$ cm³/sec (Ref. 4) is very satisfactory.

Regarding comparison to theoretical values, the “standard” effective-mass treatment¹³ depends on

TABLE III. Best Auger coefficients $B(r=1)$.

Transition probabilities	B (10^{-11} cm ³ /sec)	
	From efficiency data	From decay data (Ref. 1)
Independent of screening	2.3 ± 0.3	2 ± 0.5
Dependent on screening	3 ± 0.5	6 ± 2

wave-function overlap integrals (F 's) which are poorly known. Estimates¹⁴ for the F 's lead to $B \approx 5 \times 10^{-12}$ to 10^{-10} cm³/sec, a range fully covering the experimental values. An alternate treatment using a p -type function for the hole¹⁵ gives, when corrected for exchange terms,¹³ a value of $B \approx 10^{-10}$ cm³/sec, which is rather larger than the experimental values.

As a final comment: As just stated, the present Auger values, for a Hall factor of unity, range from 2×10^{-11} to 3.5×10^{-11} cm³/sec. For a differ-

ent Hall factor, a proportionate inverse change in Auger coefficient is obtained (see comments in Sec. IV B). Since the likeliest range of Hall factor is 0.7–1 (Ref. 1), we conclude that our "best estimate" is $B = (2-5) \times 10^{-11}$ cm³/sec.

ACKNOWLEDGMENT

The authors are indebted to Dr. S. K. Kurtz for his encouragement in this work.

¹G. F. Neumark, D. J. DeBitetto, R. N. Bhargava, and P. M. Harnack, preceding paper, Phys. Rev. B **15**, 3147 (1977).

²R. N. Bhargava, J. Appl. Phys. **41**, 3698 (1970).

³J. S. Jayson, R. N. Bhargava, and R. W. Dixon, J. Appl. Phys. **41**, 4972 (1970).

⁴J. M. Dishman and M. DiDomenico, Jr., Phys. Rev. B **1**, 3381 (1970); J. M. Dishman, M. DiDomenico, Jr., and R. Caruso, *ibid.* **2**, 1988 (1970).

⁵C. H. Henry, R. Z. Bachrach, and N. E. Schumaker, Phys. Rev. B **8**, 4761 (1973).

⁶J. A. W. van der Does de Bye and A. T. Vink, J. Luminesc. **5**, 108 (1972).

⁷J. A. W. van der Does de Bye, J. Electrochem. Soc. **123**, 544 (1976).

⁸J. S. Jayson and R. Z. Bachrach, Phys. Rev. B **4**, 477 (1971).

⁹P. T. Landsberg, C. Rhys-Roberts, and P. Lal, Proc. Phys. Soc. Lond. **84**, 915 (1964).

¹⁰C. S. Lam and Y. P. Varshni, Phys. Rev. A **4**, 1875 (1971).

¹¹Recent results by D. V. Lang [J. Appl. Phys. **45**, 3014 (1974)] gave an N_t of $(4-10) \times 10^{15}$ for well-annealed samples. The present samples were not specifically annealed, and could have slightly lower concentrations of N_t .

¹²Van der Does de Bye (Ref. 7) has concluded, on the other hand, that screening is quite important. He ev-

aluates the term fg , where g is a screening term corresponding to $(\beta/\beta_0)^3$ in our notation, and obtains $fg \sim 0.1-0.2$. His conclusion is then based on an argument that $f \sim 1$ for highly doped samples (giving $g \sim 0.1-0.2$). We have two comments on this conclusion. First, screening may indeed be important at high doping, since β/β_0 certainly decreases drastically for high screening (Ref. 10). Second, we feel van der Does de Bye overestimates the value of f (at both high and low doping). The energy reduction due to screening (included in the present paper) leads to lower f values. Thus for $p = 5 \times 10^{18}$ we estimate $E_A \lesssim 3$ meV, and $f = 0.6-0.7$ (vs $f \approx 1$ in Ref. 7). For our samples where $p = (3-9) \times 10^{17}$, we obtain $f \approx 0.1-0.25$ (Table I) vs $f \approx 0.2-0.4$ of Ref. 7. A corollary is that a good part of the low fg values (and in fact the *main* part at intermediate doping) is due to a reduction of f . In fact, in the present doping range the residual difference can be accounted for by our approach using the Lam and Varshni (Ref. 10) results; alternatively, if the absolute efficiency values of Ref. 7 are somewhat low—difficulties of accurate measurements are discussed in Ref. 7—screening may here be quite unimportant.

¹³G. F. Neumark, Phys. Rev. B **7**, 3802 (1973).

¹⁴A. R. Beattie and P. T. Landsberg, Proc. R. Soc. A **258**, 486 (1960).

¹⁵K. P. Sinha and M. DiDomenico, Jr., Phys. Rev. B **1**, 2623 (1970).